Open access • Journal Article • DOI:10.1088/0022-3727/47/13/135303

Multiferroic BaTiO 3 -BiFeO 3 composite thin films and multilayers: strain engineering and magnetoelectric coupling — Source link

Michael Lorenz, Vera Lazenka, Peter Schwinkendorf, Francis Bern ...+7 more authors

Institutions: Leipzig University, Katholieke Universiteit Leuven

Published on: 02 Apr 2014 - Journal of Physics D (IOP Publishing)

Topics: Ferroelectricity, Magnetization, Pulsed laser deposition, Thin film and Ferromagnetism

Multiferroic $BaTiO_3$–$BiFeO_3$ composite thin films and multilayers: strain engineering and magnetoelectric coupling

2014 J. Phys. D: Appl. Phys. 47 135303

IOP Publishing Journal of Physics D: Applied Physics
J. Phys. D: Appl. Phys. **47** (2014) 135303 (10pp) doi:10.1088/0022-3727/47/13/135303

Multiferroic $BaTiO_3$–$BiFeO_3$ composite thin films and multilayers: strain engineering and magnetoelectric coupling

Michael Lorenz[1,4], Vera Lazenka[2,4], Peter Schwinkendorf[1], Francis Bern[1], Michael Ziese[1], Hiwa Modarresi[2], Alexander Volodin[3], Margriet J Van Bael[3], Kristiaan Temst[2], André Vantomme[2] and Marius Grundmann[1]

[1] Institut für Experimentelle Physik II, Universität Leipzig, Linnéstraße 5, D-04103 Leipzig, Germany
[2] Instituut voor Kern- en Stralingsfysica, KU Leuven, Celestijnenlaan 200D, B-3001 Leuven, Belgium
[3] Laboratorium voor Vaste-Stoffysica en Magnetisme, KU Leuven, Celestijnenlaan 200D, B-3001 Leuven, Belgium

E-mail: mlorenz@physik.uni-leipzig.de and Vera.Lazenka@fys.kuleuven.be

Received 30 December 2013, revised 7 February 2014
Accepted for publication 11 February 2014
Published 11 March 2014

Abstract

$BiFeO_3$ and $BaTiO_3$ were used to grow homogeneous composite thin films and multilayer heterostructures with 15 double layers by pulsed laser deposition. The perpendicular strain of the films was tuned by employing different substrate materials, i.e. $SrTiO_3$(0 0 1), MgO(0 0 1) and $MgAl_2O_4$(0 0 1). Multiferroic properties have been measured in a temperature range from room temperature down to 2 K. The composite films show a high ferroelectric saturation polarization of more than 70 $\mu C\,cm^{-2}$. The multilayers show the highest magnetization of 2.3 emu cm^{-3}, due to interface magnetic moments and exchange coupling of the included weak ferromagnetic phases. The magnetoelectric coupling of the $BaTiO_3$–$BiFeO_3$ films was investigated by two methods. While the ferroelectric hysteresis loops in magnetic fields up to 8 T show only minor changes, a direct longitudinal AC method yields a magnetoelectric coefficient $\alpha_{ME} = \partial E/\partial H$ of 20.75 V cm^{-1} Oe^{-1} with a low $\mu_0 H_{DC}$ of 0.25 T for the 67% $BaTiO_3$–33% $BiFeO_3$ composite film at 300 K. This value is close to the highest reported in the literature.

Keywords: multiferroic composite, magnetoelectric coupling, $BiFeO_3$ and $BaTiO_3$, exchange coupling, multiferroic oxide, pulsed laser deposition

(Some figures may appear in colour only in the online journal)

S Online supplementary data available from stacks.iop.org/JPhysD/47/135303/mmedia

1. Introduction

Among the single-phase multiferroics, $BiFeO_3$ (BFO) is the most widely studied compound (Catalan and Scott 2009, Lawes and Srinivasan 2011), showing remarkable polarization (60 $\mu C\,cm^{-2}$) and high magnetization (up to 1 μ_B/Fe) in the strained state for film thickness below 100 nm (Wang *et al* 2003). However, BFO thin films often show high leakage currents, due to oxygen vacancies and mixed Fe valences (Pabst *et al* 2007). Consequently, the ferroelectric response as derived from current–voltage characteristics is often dominated by the resistive contribution and, therefore, extraction of the magnetoelectric (ME) coupling coefficient may be difficult (Bern *et al* 2014).

The above-mentioned high intrinsic ferroelectric polarization of BFO was confirmed by other groups (Vaz 2012). However, the intrinsic magnetization of BFO films is currently considered to be nearly zero (about 0.02 μ_B/unit cell); see the review (Catalan and Scott 2009). Furthermore, the multiferroic properties of various BFO films seem to depend critically on subtle differences in microstructure as governed by the growth process (Lawes and Srinivasan 2011, Vaz 2012). In this regard,

[4] Authors to whom any correspondence should be addressed.

the groups of the authors succeeded in increasing the magnetic response of heteroepitaxial BFO films by Gd doping, and found a clear ferroelectric response by piezoresponse force microscopy (PFM) (Lazenka *et al* 2013).

To overcome the limitations of single-phase multiferroics, composite and multilayer multiferroics consisting of coupled magnetic and ferroelectric phases are promising to show higher magnetization values up to the order of tens of emu cm^{-3} (in SI units, 1 emu cm^{-3} = 10^3 A m^{-1}, corresponding to $\mu_0 M = 4\pi \times 10^{-4}$ T), and polarization up to tens of μC cm^{-2} (10^{-2} C m^{-2}), respectively (Lawes and Srinivasan 2011). For example, multiferroic $ZnFe_2O_4/BaTiO_3$ (ZFO/BTO) composite thin films show a magnetization of 8 and 30 emu cm^{-3} for the ZFO/BTO multilayer; and ferroelectric polarization around 8 μC cm^{-2} (Lorenz *et al* 2012). However, the magnetodielectric coupling in the ZFO/BTO composite films was found to be weak, of the order of 0.01% and 0.8% for the real and imaginary parts of the permittivity, respectively.

In general, the ME coupling in multiferroic heterostructures can be mediated by strain, or exchange interaction, or can be induced by charge transport (Vaz 2012). A prototype system for strain-mediated ME coupling is the $CoFe_2O_4$–BTO nanocomposite, with sharp drops of magnetic moment at the structural phase transition temperature of BTO (Liu 2010). The coefficient $\alpha_H = \partial H/\partial E$ of the inverse ME coupling (electric-field-induced changes of the magnetization) of various oxide-based multiferroic heterostructures is of the order of 500 to 10^5 Oe cm V^{-1} (Vaz 2012). However, the highest magnetic-field-induced voltage coefficient $\alpha_{ME} = \partial E/\partial H$ = 22 V cm^{-1} Oe^{-1} (in SI units, 1 V cm^{-1} Oe^{-1} = $4\pi \times 10^{-1}$ V A^{-1}) at low frequency (f = 1 kHz) is reported for a FeBSiC/$PbZr_{1-x}Ti_xO_3$-fibre laminate with a resonance enhancement to 500 V cm^{-1} Oe^{-1} at 20 kHz (Dong *et al* 2006).

Only a few BFO-containing composites have been investigated up to now: (a) strain-mediated composite nanostructures BFO with $CoFe_2O_4$ (Zavaliche *et al* 2005, Zheng *et al* 2006, Dix *et al* 2009, Aimon *et al* 2012), $NiFe_2O_4$ (Zhan *et al* 2006) or Fe_3O_4 (Weal *et al* 2010); (b) exchange-mediated multiferroics with electric field control of exchange bias in BFO with FeCo (Chu *et al* 2008), $Ni_{78}Fe_{22}$ or (LaSr)MnO_3 (Wu *et al* 2010) and (c) combinations of BFO with another ferroelectric phase such as BTO: BFO/BTO multilayers showed an increased magnetization with double number of interfaces in structures with identical total thickness (Toupet *et al* 2008). Substitution of BFO by (NdBi)FeO_3 and BTO by $BaSrTiO_3$ in the multilayers results in even higher magnetization, up to 60 emu cm^{-3} (Ivanov *et al* 2012). Polycrystalline Ba-doped BFO thin films with preferential (1 0 1) orientation showed a weak polarization of 4.8 μC cm^{-2} and a magnetization of 3.3 emu g^{-1} at 300 K, together with a magnetodielectric coupling of 1.1% at an 8 kOe magnetic field at 10 kHz (2007).

In order to explore the obvious sensitivity of the multiferroic properties of BFO-based materials to the growth process and the resulting microstructure, we have conducted systematic investigation of composite thin films and multilayers built from BFO and BTO phases. The composite films and multilayers grown by pulsed laser deposition (PLD) show clear ferroelectric and weak ferromagnetic responses. ME effects were measured using two different methods. First, ferroelectric polarization hysteresis measurements $P(E, B)$ were made in magnetic fields up to 8 T. Second, the ME coefficient α_{ME} was directly determined by measuring the induced AC voltage upon application of an AC magnetic field in longitudinal geometry.

Table 1. Overview of investigated films grown on $SrTiO_3$(0 0 1), i.e. film material, PLD oxygen partial pressure $p(O_2)$ and particular film thickness as determined by RBS, and minimum channelling yield as an estimate of the crystalline quality near the surface; see figure 1 for selected RBS spectra. The error bar of thickness is around ±8 nm.

Film material	Sample no	$p(O_2)$ (mbar)	Thickness (μm)	RBS/C χ_{min} (%)
$BaTiO_3$ (BTO)	G4150	0.25	0.680	4
	G4154	0.01	1.750	35
$BiFeO_3$ (BFO)	G4159	0.25	0.470	8
	G4163	0.01	0.800	9
15× BTO/BFO multilayer	G4172	0.25	0.440	20
	G4176	0.01	1.300	25
BTO67/BFO33 composite	G4182	0.25	0.830	14
	G4186	0.01	1.850	24
BTO33/BFO67 composite	G4190	0.25	0.600	28
	G4194	0.01	1.500	7

2. Experimental set up

Thin-film samples of five different types were grown by PLD. These are the single-phase films (a) BTO and (b) BFO, (c) multilayers of 15 BTO/BFO double layers and (d), (e) composites grown directly from mixed PLD targets with 67 wt% BTO/33 wt% BFO (in the following referred to as BTO67/BFO33) and 33 wt% BTO/67 wt% BFO (BTO33/BFO67), respectively (table 1). The single-phase and composite PLD targets were prepared from 5N $BaTiO_3$, Bi_2O_3 and Fe_2O_3 powders (Alfa Aesar) and sintered in air for 6 h at 1200 °C (composites), 6 h at 1300 °C (BTO) or twice for 12 h at 810 °C (BFO).

The PLD film growth was carried out simultaneously on four different substrate materials, namely $SrTiO_3$(0 0 1) (STO), $SrTiO_3$: 0.5%Nb(0 0 1) (STO : Nb), MgO(0 0 1) and $MgAl_2O_4$(0 0 1), using a rotating substrate holder with positions for four 5×5 mm^2 substrates. The substrate holder is slightly offset from the centre of the plasma plume to ensure a homogeneous deposition on the four substrates (Lorenz 2008). Each of the five film types was grown with two different oxygen partial pressures, 0.25 and 0.01 mbar; see table 1. The growth temperature was 680 °C, and 300 laser pulses at 1 Hz plus 30 000 subsequent pulses at 15 Hz were applied for all films. For the multilayers, 1000 pulses were applied for one single layer, i.e. also 30 000 pulses in total for 15 double layers. For more details of the PLD methods see (Lorenz 2008, Lorenz and Rao 2014).

Random and channelling Rutherford backscattering spectrometry (RBS and RBS/C) was performed using a 1.57 MeV $^4He^+$ beam with the sample mounted on a three-axis goniometer. The composition and thickness of the films were

obtained by fitting the RBS spectra using the RUMP simulation software (Doolittle 1985).

Atomic force microscopy (AFM) surface images were taken using a Park XE-150 system in dynamic noncontact mode. Scanning electron microscopy (SEM) images were taken during preparation of cross sections in a field emission electron microscope with focused ion beam (FEM-FIB) Nova NanoLab 200 from FEI.

Wide-angle x-ray diffraction patterns were recorded with a Philips X'pert diffractometer using Cu Kα radiation and a Bragg–Brentano goniometer with focusing beam optics with a graphite secondary monochromator. Reciprocal space maps around symmetric and asymmetric substrate peaks were measured with a PANalytical X'pert MRD PRO diffractometer with parabolic mirror and PIXcel^{3D} detector.

The multiferroic properties, i.e. the magnetic and ferroelectric hysteresis, were investigated by measurements with SQUID (superconducting quantum interference device) magnetometers (Quantum Design MPMSXL-5 in Leuven, and Quantum Design MPMS-7 in Leipzig). In all measurements, the magnetic field is applied parallel to the surface of the films. Also, ferroelectric polarization hysteresis measurements were carried out using the thin-film analyser TF 2000 HS (aixACCT) at room and low temperatures. The dynamic hysteresis mode with triangular excitation pulses and with internal leakage compensation was used. The measurement frequency was 1 or 2 kHz. Capacitor structures with conducting STO : Nb substrates and DC-sputtered Pt top contacts of diameter 225 μm were used for the latter measurements.

In addition, the ferroelectric properties of the samples were probed by PFM (Hong *et al* 2001). PFM measurements were made at ambient conditions with a Dimension 3100 microscope from Bruker. PFM images were acquired in contact mode at 30 kHz, with AC voltage amplitudes of 2–5 V using PPP-EFM probes from NanoAndMore with PtIr coating.

The ME coupling, i.e. the change in ferroelectric response on applying a magnetic field, was first investigated by performing the above-mentioned ferroelectric hysteresis measurements in a He flow cryostat (Oxford Instruments) with a superconducting solenoid providing a magnetic field up to 8 T, at selected sample temperatures of 10, 50 and 100 K. In all measurements, the magnetic field was parallel to the thin-film capacitors.

Second, the ME coefficient α_{ME} (equation (1)) was determined as a function of DC magnetic field and temperature using a Quantum Design physical property measurement system.

$$\alpha_{\mathrm{ME}} = \frac{\mathrm{d}E}{\mathrm{d}H} = \frac{1}{t}\frac{\mathrm{d}V}{\mathrm{d}H} = \frac{1}{t}\frac{V_{\mathrm{AC}}}{H_{\mathrm{AC}}}. \qquad (1)$$

where t is the thickness of the films. The AC voltage induced across the capacitor structures in response to a small AC magnetic field with $f = 1$ kHz and $H_{\mathrm{AC}} = 10$ Oe ($1\,\mathrm{Oe} = 10^3/4\pi\,\mathrm{A\,m^{-1}}$) was measured using a lock-in amplifier (Stanford Research System, SR830). Both DC and AC magnetic fields were applied across the sample along the ME voltage, i.e. in longitudinal geometry (Lazenka *et al* 2012). The sensitivity of the setup was tested by comparing the voltage response of a $LiNbO_3$/Fe bilayer with that of our 15 × BFO/BTO multilayer G4177. While the voltage response of the ferroelectric $LiNbO_3$ structure was a few microvolts only (i.e. no sizable ME coupling), our multiferroic BTO/BFO multilayer of similar dimension generated a few millivolts response.

3. Sample composition and crystalline structure

The film composition, crystalline quality, film orientation and out-of-plane lattice constants were systematically investigated with RBS/C and XRD. Figure 1 shows random and aligned RBS spectra of (*a*) the BTO33/BFO67 composite film and (*b*) the 15× BTO/BFO multilayer. The backscattering yield was normalized to the measurement geometry, i.e. the spatial angles and collected charge. The film thickness as determined from the RUMP simulation can be found in table 1, together with the minimum channelling yield χ_{min} for all samples. The latter quantity is a measure for the crystallinity of the sample, with values ranging from a few per cent (perfect single crystal) to 100% (polycrystalline). Given the 15 keV RBS detector energy resolution, a ±8 nm thickness error has been calculated for all samples.

Figure 1(*c*) shows an SEM image of a cross section of a 15× BTO/BFO multilayer, together with AFM surface images of the two different composite film types. The multilayer shows smooth surface and interfaces; the typical rms surface roughness (R_{rms}) of a multilayer is around 1 nm. As the AFM images show, the composite films are rougher, with R_{rms} up to 8.5 nm, indicating a granular structure of the BTO and BFO phases. Typical grain and nanoparticle sizes of the composite films are in the ranges 40–100 nm and 100–200 nm, respectively; see figure 1(*c*). These are typical values found also for other nanocomposites with strain-mediated ME coupling, such as $CoFe_2O_4$–BTO (Liu 2010).

If we compare films grown at different PLD oxygen pressures, the strongly decreased deposition rate at 0.25 mbar is obvious, due to higher scattering and slowing down of the plasma constituents in the background oxygen. Interestingly, the crystalline perfection of the BTO33/BFO67 composite film is much better for the lower growth pressure, as indicated by the minimum yields in table 1. For all other films the 0.25 mbar samples show lower χ_{min} values, due to larger grain size and smaller oxygen vacancy concentration. From the good agreement of the RBS simulation and experiment, we conclude that the composition of the films is very close to stoichiometric. We cannot exclude a weak deficiency of Bi, but this is limited to 5–6% at most. In addition, there is no obvious difference in composition for films grown at 0.25 or 0.01 mbar PLD oxygen pressure.

The XRD 2Θ–ω diffraction patterns in figure 2 show the (0 0 2) substrate peaks of (*a*) $SrTiO_3$, and (*b*) MgO, together with the corresponding film peaks. Except for the multilayers, the samples show one dominating crystalline phase in preferential (0 0 1) orientation. The corresponding out-of-plane lattice constants of the films as calculated from the (0 0 2) peak positions are listed in table 2. The lattice constants show a remarkable variation, although the films were grown simultaneously on the different substrate materials.

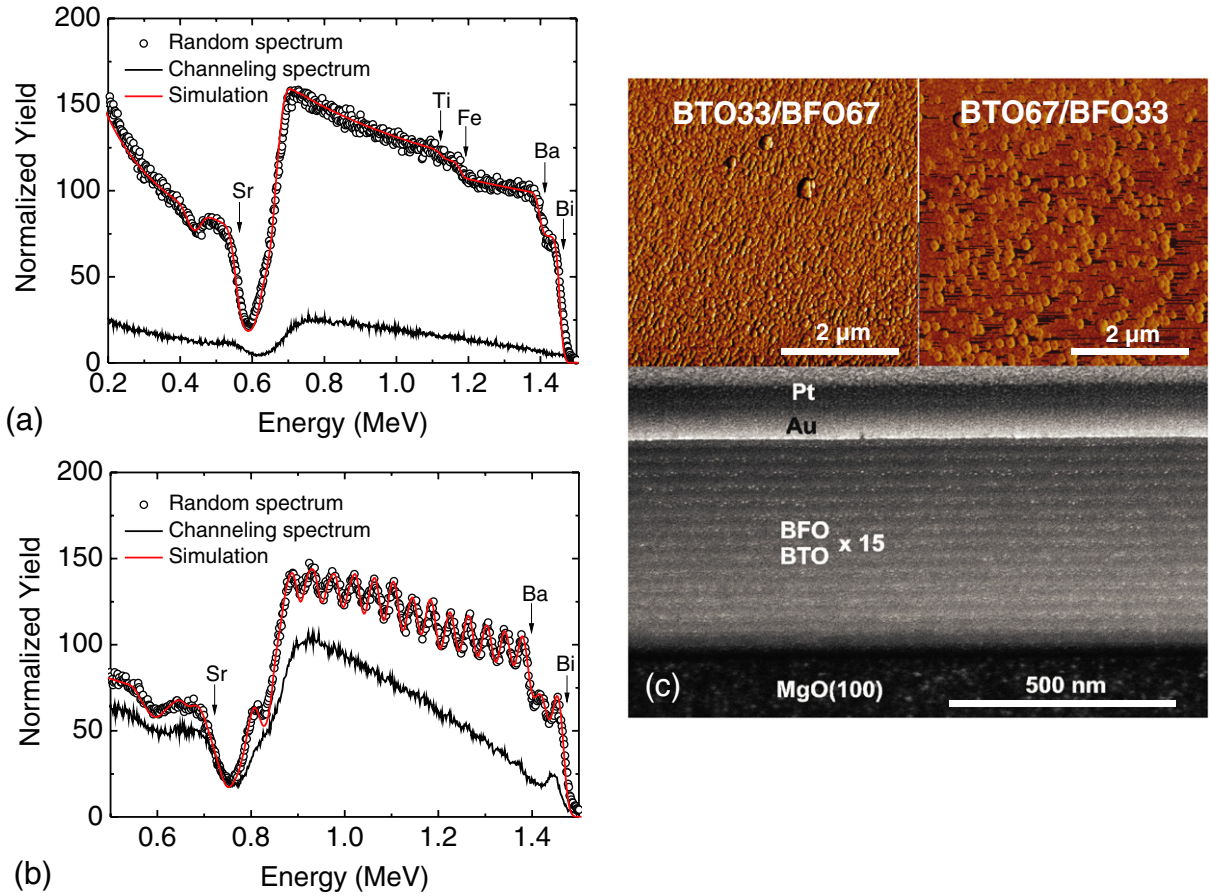

Figure 1. Random and channelling RBS spectra of (*a*) BTO33/BFO67 composite film and (*b*) 15× BTO/BFO multilayer, both grown at 0.01 mbar on $SrTiO_3$(0 0 1). The latter spectrum shows the repetitive superposition of Bi and Ba element contributions of alternating layers. More RBS spectra can be found in the online supplementary information (stacks.iop.org/JPhysD/47/135303/mmedia). (*c*) SEM image of the cross section of a 15× BTO/BFO multilayer on MgO (0.01 mbar), demonstrating the smooth interfaces of the single BTO (dark) and BFO (with white granular contrast) layers. Au and Pt top layers are added to support the preparation in the FEM-FIB. On top are shown AFM surface images of the two types of composite film as indicated, grown at 0.25 mbar. The corresponding R_{rms} values are as follows: BTO33/BFO67 6.1 nm; BTO67/BFO33 8.4 nm; multilayer 1.07 nm (AFM image of multilayer in supplementary information).

Nearly all films listed in table 2 show a slightly decreasing lattice constant in the order STO (3.905 Å), MgO (4.212 Å), $MgAl_2O_4$ (8.081 Å), because the cubic in-plane lattice constant increases in the same order. Reciprocal space maps around the asymmetric (−1 0 3), (−1 1 3) and (−1 1 4) substrate peaks did not confirm a fully pseudomorphic, i.e. in-plane lattice-matched, film growth for the BTO67/BFO composite on STO.

The oxygen pressure dependence in table 2 reflects the usual behaviour of lattice widening with lower oxygen growth pressure, due to increasing density of oxygen vacancies. This effect is most pronounced for BTO and for both the BTO67/BFO33 and the BTO33/BFO67 composites. In contrast, single-phase BFO films on all substrates show decreasing lattice constants with lower pressure. BFO exhibits a rhombohedral crystal structure, unlike the other involved compounds, which are cubic.

4. Multiferroic properties

All thin-film samples show both weak ferromagnetic and ferroelectric behaviour, i.e., they can be considered as multiferroic. The magnetic hysteresis loops measured at 300 K and 2 K are presented in figures 3 and 4, respectively. The measured M–H loops confirm the ferromagnet-like behaviour of the films. The ferromagnetic order appears because the thin-film geometry suppresses the incommensurate spiral spin structure of bulk BFO (Sosnowska *et al* 1982, Wang *et al* 2003). The hysteresis loops present characteristics typical of a soft magnetic phase with a low coercive field $\mu_0 H_C$ of about 0.05 T at room temperature for the BFO film and 0.085 T for the multilayer grown at 0.25 mbar. It is known (Wang *et al* 2003) that the magnetization value in BFO increases when the film thickness decreases due to increased lattice mismatch strain. Interestingly, the saturation magnetization M_S of the multilayer is substantially larger than that of the single-phase BFO and the composite thin films, while the M_S values for the single-phase BFO and composite BTO67/BFO33 and BTO33/BFO67 films are almost identical. This tendency remains for the samples grown at 0.01 mbar but with about 50% smaller saturation magnetization (not shown here). This result is in good agreement with the observations made by (Toupet *et al* 2008). Toupet showed that the magnetization in BTO/BFO multilayers increases when the number of interfaces in the superlattice increases. Obviously,

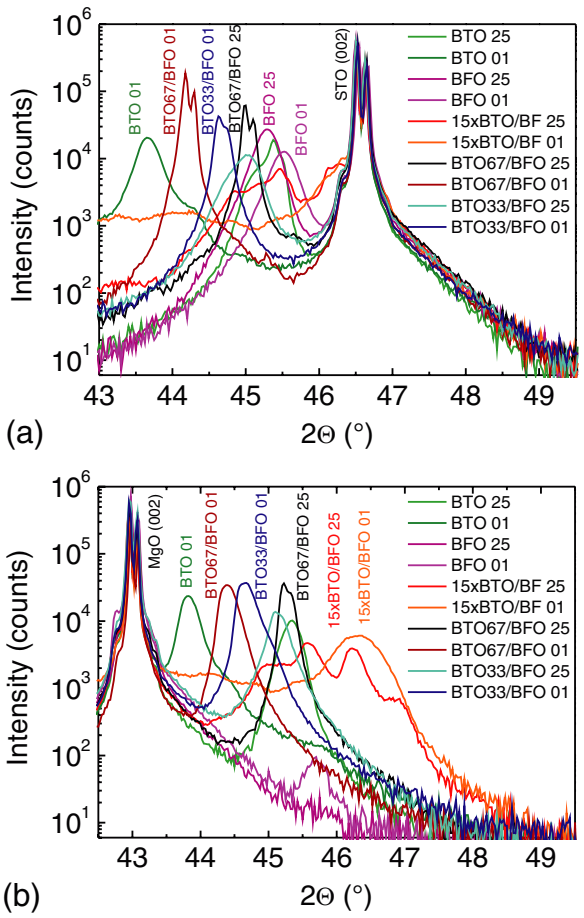

Figure 2. XRD 2Θ–ω diffraction peaks of films near the (0 0 2) substrate peaks of (*a*) $SrTiO_3$(0 0 1) and (*b*) MgO(0 0 1). BTO 25 stands for $BaTiO_3$ grown at 0.25 mbar, and BFO 01 for $BiFeO_3$ at 0.01 mbar. For the XRD patterns of films on $MgAl_2O_4$(0 0 1) and reciprocal space maps see the online supplementary information (stacks.iop.org/JPhysD/47/135303/mmedia).

the enhancement of magnetization originates at the BFO/BTO interfaces. Probably, defect states at the interfaces are responsible for the clearly increased saturation magnetization of the multilayers in figures 3 and 4; see the current discussion of defect-induced magnetic signals in (Zippel *et al* 2013) and references therein.

As shown in figure 3, single-phase BTO films also show a weak ferromagnetic signal. This effect has already been observed in nanocrystalline BTO samples (Ding and Zhou 2011, Cao *et al* 2009, Sundaresan and Rao 2009) and is found to be induced by oxygen and titanium vacancies. In our previous work (Lorenz *et al* 2012), we found for the single-phase BTO film a similar magnetic signal, and this defect-induced magnetism is now established for other nominal nonmagnetic oxide thin films such as undoped ZnO (Khalid *et al* 2009) and ZrO_2 (Zippel *et al* 2013). Therefore, both BFO and BTO layered phases possess weak net magnetic moments. Therefore, the spin alignment at the interface may result in a weak ferromagnetic coupling and thus an additionally increased magnetic moment in the BTO/BFO multilayers in comparison with the composite films. Magnetic hysteresis loops measured at 2 K (figure 4) follow the same tendency

Table 2. XRD out-of-plane lattice constants for films on the following substrates: $SrTiO_3$(0 0 1) with $a = 3.905$ Å, MgO(0 0 1) with $a = 4.212$ Å and $MgAl_2O_4$(0 0 1) with $a = 8.081$ Å, calculated from the (0 0 2) film peak position. The uncertainty of the lattice constants due to the goniometer height error is about 0.003 Å. The bulk values for BTO and BFO in the first column are taken from JCPDS v.2.0 files 83–1877 and 74–2016, respectively.

Film material lattice const.	$p(O_2)$ (mbar)	c (Å) on $SrTiO_3$(0 0 1)	c (Å) on MgO(0 0 1)	c (Å) on $MgAl_2O_4$(0 0 1)
$BaTiO_3$ (BTO)	0.25	3.994	3.997	3.989
$c = 4.033$ Å	0.01	4.146	4.129	4.067[a]
$BiFeO_3$ (BFO)	0.25	4.004	3.988[a]	3.945
$a = 3.962$ Å	0.01	3.985	3.967	3.943
15× BTO/BFO	0.25	3.990	3.924[a]	4.028[a]
multilayer	0.01	4.094[a]	3.919	3.908
BTO67/BFO	0.25	4.026	4.006	3.997
composite	0.01	4.097	4.078	4.043
BTO33/BFO	0.25	4.027	4.016	4.001
composite	0.01	4.057	4.056	4.037

[a] Multiple or broad peaks, or calculated from (0 0 1) peak.

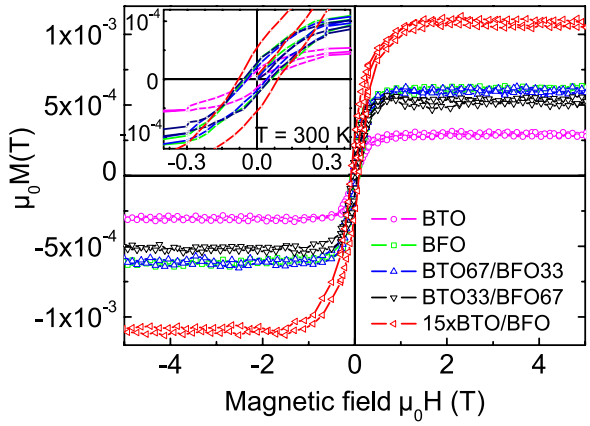

Figure 3. Magnetic hysteresis of the indicated films grown at 0.25 mbar on $SrTiO_3$ measured by SQUID at 300 K. The inset is an enlargement of the central part of the figure. The maximum saturation magnetization of the multilayer in CGS units is about 0.85 emu cm^{-3}.

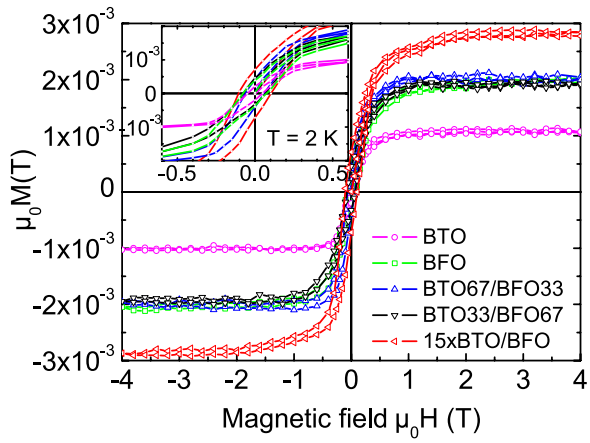

Figure 4. Magnetic hysteresis of the films grown at 0.25 mbar on $SrTiO_3$ measured by SQUID at 2 K. The inset shows the opening of all hysteresis loops, i.e. ferromagnetism. The maximum saturation magnetization of the multilayer in CGS units is about 2.3 emu cm^{-3}.

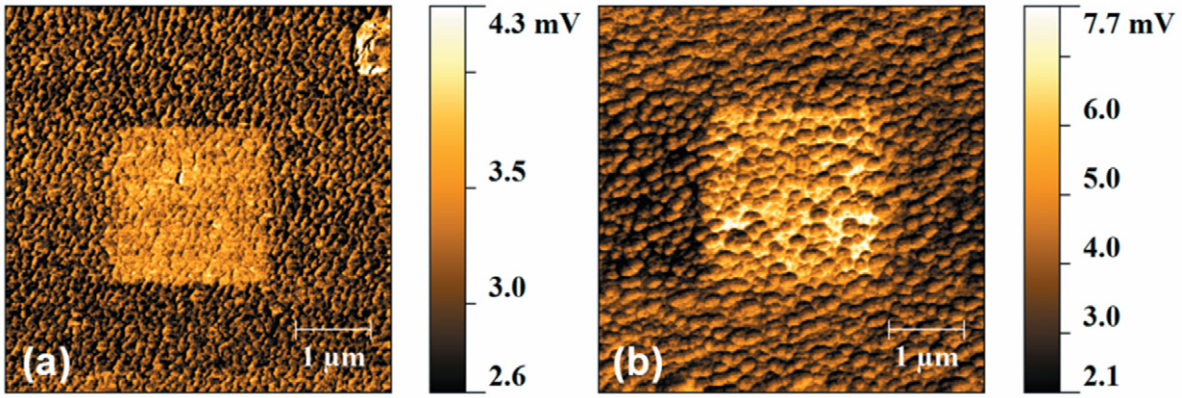

Figure 5. PFM images acquired at 300 K of (*a*) BTO33/BFO67 (G4727d) and (*b*) BTO67/BFO33 (G4728c), both grown at 0.25 mbar and on STO : Nb, after poling of the central square region (bright square) with (*a*) −10 V and (*b*) −12 V.

as room-temperature loops (figure 3), but with enhanced magnetic characteristics M_S and H_C. This is consistent with our previous work (Lazenka *et al* 2013), where an increase of magnetization with decreasing temperature in BFO thin films was shown.

The remarkable ferroelectric properties of the samples are demonstrated in figures 5 and 6. Figures 5(*a*) and (*b*) show the PFM images of the BTO33/BFO67 and the BTO67/BFO33 composite films, respectively, after poling the bright square regions during scans with DC voltage biases of −10 V or −12 V applied to the PFM tip, as indicated. Before poling, the samples show no preferential ferroelectric orientation. A possible reason for the absence of the piezoresponse contrast is the following. Since the films are sufficiently thick (see table 1), small and randomly polarized grains may be stacked in the direction normal to the film plane. The piezoresponses of these grains will cancel each other, leading to negligible integral piezoresponse (Gruverman *et al* 1998). Note that larger size (up to micrometres) spontaneous ferroelectric domains were observed in high-quality 2–120 nm thick BFO samples (Chu *et al* 2007). The poling of the square region results for both composite films in a clear ferroelectric orientation, as visualized by the PFM response in figure 5. Obviously, the BTO67/BFO33 composite (b) shows a higher PFM signal compared to the BTO33/BFO67 composite (a). This is in agreement with the ferroelectric hysteresis loops of these samples in figures 6(*c*) and (*e*). The PFM contrast image remained almost the same for many hours (>12 h) after the polarization, indicating the high ferroelectric quality of our composite films.

Figure 6 shows selected ferroelectric hysteresis loops together with the *I*–*V* curves taken at 1 kHz for (*a*) the BTO film, (*b*) the BTO/BFO multilayer, (*c*), (*d*) the BTO67/BFO33 composite thin film and (*e*), (*f*) the BTO33/BFO67 composite film. The composites were measured at both 300 K and 50 K as indicated. The particular film thickness (see table 1) was taken into account for the conversion of the applied voltage to electric field units. Additional ferroelectric data of the BTO film (0.01 mbar), a BFO film (0.25 mbar) and the BTO33/BFO67 composite film (0.01 mbar) samples can be found in the online supplementary information (stacks.iop.org/JPhysD/47/135303/mmedia).

In general, the ferroelectric response of the samples can be distinguished as follows:

(a) the BTO films and the BTO67/BFO33 and the BTO33/BFO67 composites grown at 0.25 mbar show very good ferroelectric response, as shown in figures 5 and 6;
(b) the BFO films and the composites grown at 0.01 mbar show higher leakage current or not clearly resolved ferroelectric current switching peaks, and could be measured only at 50 K; see figure 6(*b*);
(c) a few samples such as the BFO film and the BTO67/BFO33 composite grown at 0.01 mbar, and the multilayer deposited at 0.25 mbar, show very high leakage or almost no ferroelectric response. This may be due to oxygen deficiency resulting from the 0.01 mbar growth pressure or the enhanced roughness of the multilayer at 0.25 mbar.

The BTO67/BFO33 composite shows particularly good ferroelectric properties; see figures 5(*b*) and 6(*c*), (*d*). In this context we mention that iron doping of $Sr_xBa_{1-x}TiO_3$ has remarkably enhanced the quality factor of polycrystalline capacitor structures for varactor applications (Lorenz *et al* 2003). More details of the performance of this BTO67/BFO33 composite sample G4183, which is beyond the scope of this paper, are given in the online supplementary information, such as the frequency and temperature dependence of the ferroelectric polarization.

5. Magnetoelectric coupling

The electric field control of magnetism or magnetically controlled ferroelectric order in the solid state is significant both fundamentally and practically, but remains a challenge. So far the only known intrinsic room temperature ME material is bismuth ferrite, BFO. However, the origin of ferroelectricity in single-phase multiferroics is largely unrelated to the magnetic order, and the ME coupling so far observed at room temperature in these materials is still too weak to be useful for device design (Wang *et al* 2003, Lazenka *et al* 2012).

As mentioned above, an alternative and promising way towards the development of ME systems is the use of

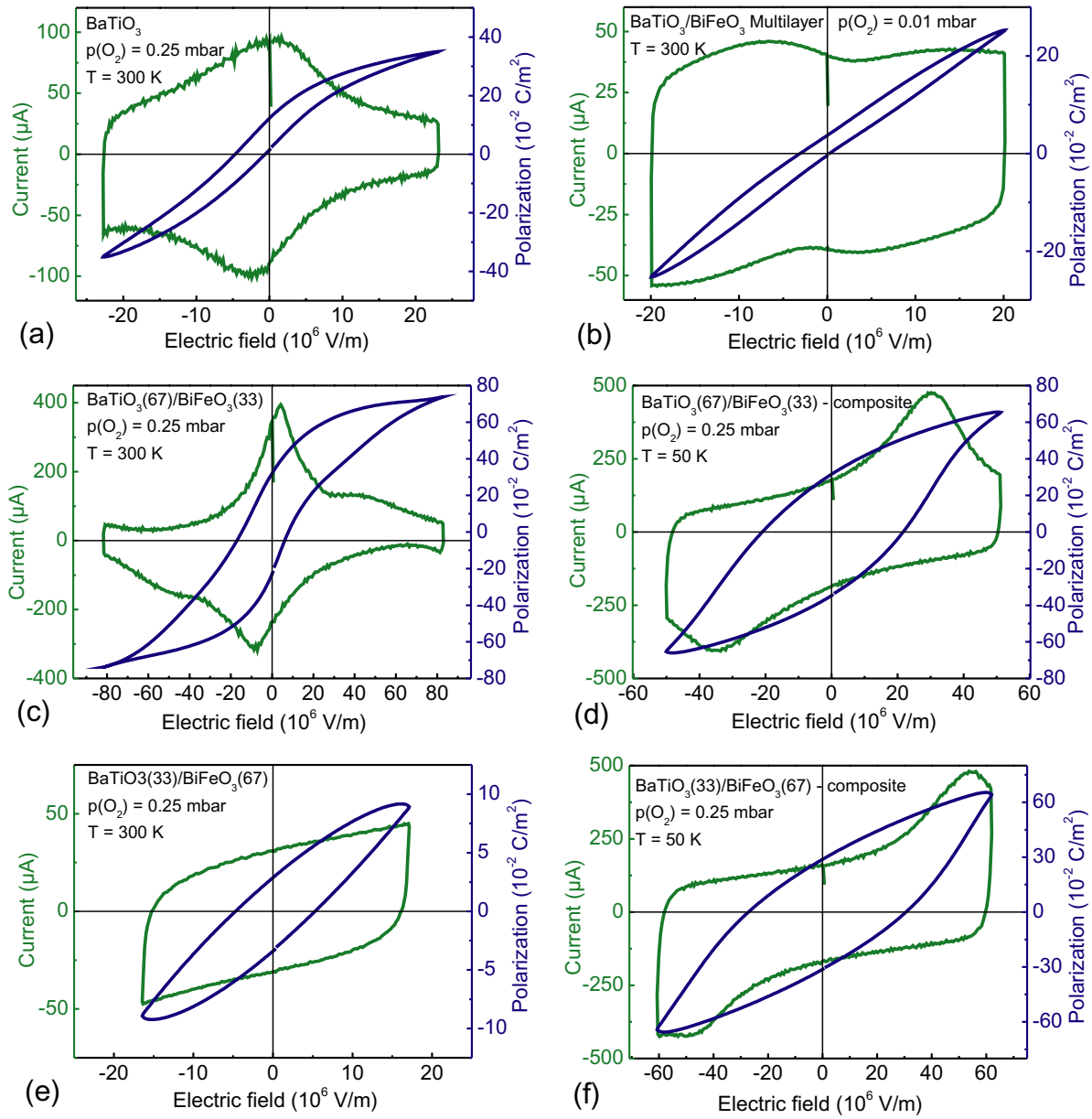

Figure 6. Ferroelectric hysteresis of (*a*) $BaTiO_3$, (*b*) 15× BTO/BFO multilayer, (*c*), (*d*) BTO67/BFO33 composite and (*e*), (*f*) BTO33/BFO67 composite thin film taken at the indicated temperatures. The composites show very high electric field stability and high saturation polarization (*c*), (*d*), (*f*).

artificial two-phase systems consisting of ferromagnetic and ferroelectric materials (Vaz 2012). In this case, the ME effect results from the interaction between different orderings of the two phases in the composite. This is an interface coupled electrical and magnetic ordering via elastic interaction between the piezoelectric and piezomagnetic phases (Ma *et al* 2011).

Figure 7 shows a typical ferroelectric polarization loop of the sample inserted in the flow cryostat with a superconducting magnet. Similar results were obtained for both composite samples, multilayer and BFO films in magnetic fields up to 8 T and temperatures in between 50 and 200 K. Only minor changes of the hysteresis loop (the I–V characteristics) could be detected when sweeping the magnetic field from 0 to +8 T, and back to 0 and −8 T, and to 0 T. A further difficulty is to separate the minor changes of the hysteresis loops, as shown in the insets of figure 7, from minor drifts of the sample temperature because of a varying He flow due to decreasing liquid He level in the cryostat. Consequently, a clear statement about the size of the ME effect in the BTO/BFO samples is not possible from these experiments.

Therefore, a more direct method was employed to measure the ME coupling directly. Figure 8 illustrates the ME coefficient α_{ME} as a function of (*a*), (*c*) static magnetic field H_{DC} at 300 K and (*b*), (*d*) temperature for the 15× BTO/BFO multilayer and BTO33/BFO67 composite films grown at 0.01 and 0.25 mbar.

The data presented in figure 8(*a*) show that α_{ME} of the multilayer is notably larger than that of the composite. Moreover, the ME response of the multilayer and composite films differs as the magnetic field increases. For the composite

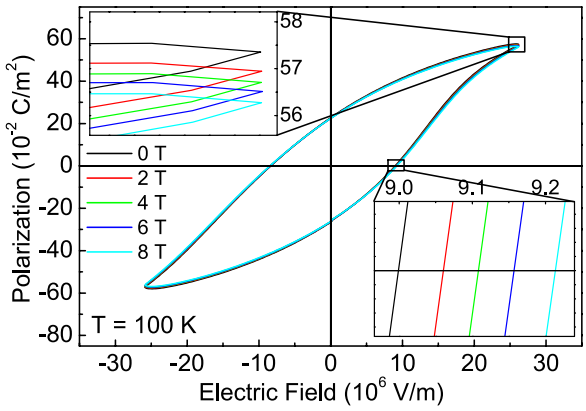

Figure 7. Ferroelectric polarization loops at $T = 100$ K of the BTO67/BFO33 composite film G4183 in dependence on magnetic field up to 8 T. This sample was measured also at 50 K and 10 K; see the online supplemental information (stacks.iop.org/JPhysD/47/135303/mmedia).

film containing 33% BFO, α_{ME} increases first to a maximum of 1.61 V cm^{-1} Oe^{-1} around 1 T and then decreases (*a*). This α_{ME} behaviour is in agreement with earlier observations for bulk BFO (Caicedo *et al* 2008, Lazenka *et al* 2012) and BFO thin films (Wang *et al* 2003). As for the multilayer, after reaching a maximum of 8.76 V cm^{-1} Oe^{-1} at 3.5 T, the ME coefficient saturates with further field increase. This α_{ME} behaviour is consistent with that found in bulk BFO samples doped with 15 and 20 at% Gd (Lazenka *et al* 2012).

Besides the intrinsic ME coupling in BFO, an additional ME effect in multilayer and composite multiferroic films is created at the interfaces. There is an elastic coupling at the interface: an applied magnetic field produces an elastic strain in the magnetostrictive phase (BFO), which is stress coupled to that of the piezoelectric (BTO), resulting in an induced voltage. Moreover, it has been shown by Bary'achtar *et al* that an electric polarization appears in the vicinity of the inhomogeneous magnetic media due to the lowering of the magnetic symmetry group of the crystal (Bary'achtar *et al* 1983). In this context, the absence of a symmetry centre in the near-interface layers should lead to an extra ME effect at the interfaces in the multilayer sample. Not only the ME coefficient α_{ME}, but also the saturation magnetization in the BTO/BFO multilayer, is larger compared to those of the composite films, as shown in figures 3 and 4.

The ME coupling in the BTO67/BFO33 composite film grown at 0.25 mbar is much higher than that at 0.01 mbar and reaches a maximum value of 20.75 V cm^{-1} Oe^{-1} at a lower $\mu_0 H_{DC}$ of 0.25 T; see figure 8(*c*). This value is close to the highest observed ME coefficient of 22 V cm^{-1} Oe^{-1} for an FeBSiC/PZT-fibre laminate (Dong *et al* 2006) at room temperature. Again, the magnetization values of these films follow a similar trend concerning oxygen partial pressure during growth.

The variation of ME coefficient with temperature is shown in figures 8(*b*) and (*d*). As temperature increases, the α_{ME} of composite films decreases more rapidly for samples grown at lower oxygen pressure. In case of the multilayer, the α_{ME} first decreases with increasing temperature from 3 to 50 K and then gradually increases up to room temperature. However, in the bulk BFO the ME coefficient gradually increases within the whole temperature range (Lazenka *et al* 2012).

6. Conclusions

Homogeneous composite thin films with 33/67 and 67/33 mixing ratios and multilayers were grown using $BaTiO_3$ and $BiFeO_3$ source compounds. The total thickness of the films ranges between 440 and 1850 nm and was shown to be highly dependent on oxygen partial pressure during PLD growth. The out-of-plane lattice constant of the films expresses strain, which was controlled using $SrTiO_3$(0 0 1), MgO(0 0 1) and $MgAl_2O_4$(0 0 1) substrate materials. All investigated samples showed weak ferromagnetic response in SQUID measurements. Capacitor structures of the BTO67/BFO33 composite on $SrTiO_3$: Nb conducting substrate showed very good ferroelectric response, with a saturation polarization of up to 75 μC cm^{-2} at 300 K and 65 μC cm^{-2} at 50 K, with high voltage stability (65 V, i.e. 80 kV mm^{-1} for a 830 nm thin film).

The ME coupling was investigated using two different approaches. First, ferroelectric hysteresis measurements were made with the samples inside a superconducting coil in a He flow cryostat. Only minor changes of the hysteresis loops were observed in static magnetic fields up to 8 T in four different samples. Both the coercive field and the average permittivity of the BTO67/BFO33 composite film changed by about 2% from 0 to 8 T.

In a second approach, we measured the longitudinal AC voltage in response to the applied AC magnetic field as a function of both DC bias magnetic field and temperature. The ME coefficient in the BTO67/BFO33 composite film grown at 0.25 mbar oxygen partial pressure is much higher than that of the similar film grown at 0.01 mbar and reaches a maximum value of 20.75 V cm^{-1} Oe^{-1} under a relatively low $\mu_0 H_{DC}$ of 0.25 T. This value is very close to the highest reported for a FeBSiC/PZT-fiber laminate. For comparison, the maximum ME coefficient of bulk BFO was measured using the same equipment and the same conditions to be 7.15 mV cm^{-1} Oe^{-1} for undoped BFO. Caicedo *et al* published 7 mV cm^{-1} Oe^{-1} for undoped BFO (Caicedo *et al* 2008). Thus the presented results prove a remarkable enhancement of the ME response of the BTO/BFO composite thin films.

Acknowledgments

We are indebted to Gabriele Ramm for preparing the PLD targets, to Holger Hochmuth for growing the PLD thin films and to Monika Hahn for preparing electrical contacts. Jörg Lenzner prepared cross sections with FIB and took SEM images. Financial support from the Deutsche Forschungsgemeinschaft within the SFB 762 'Functionality of oxide interfaces', of the European Social Fund (ESF) and the Leipzig School of Natural Sciences BuildMoNa (GS 185) is gratefully acknowledged. Work at KU Leuven was supported by the Research Foundation Flanders (FWO) and the Concerted Research Actions GOA/09/006 and GOA/14/007.

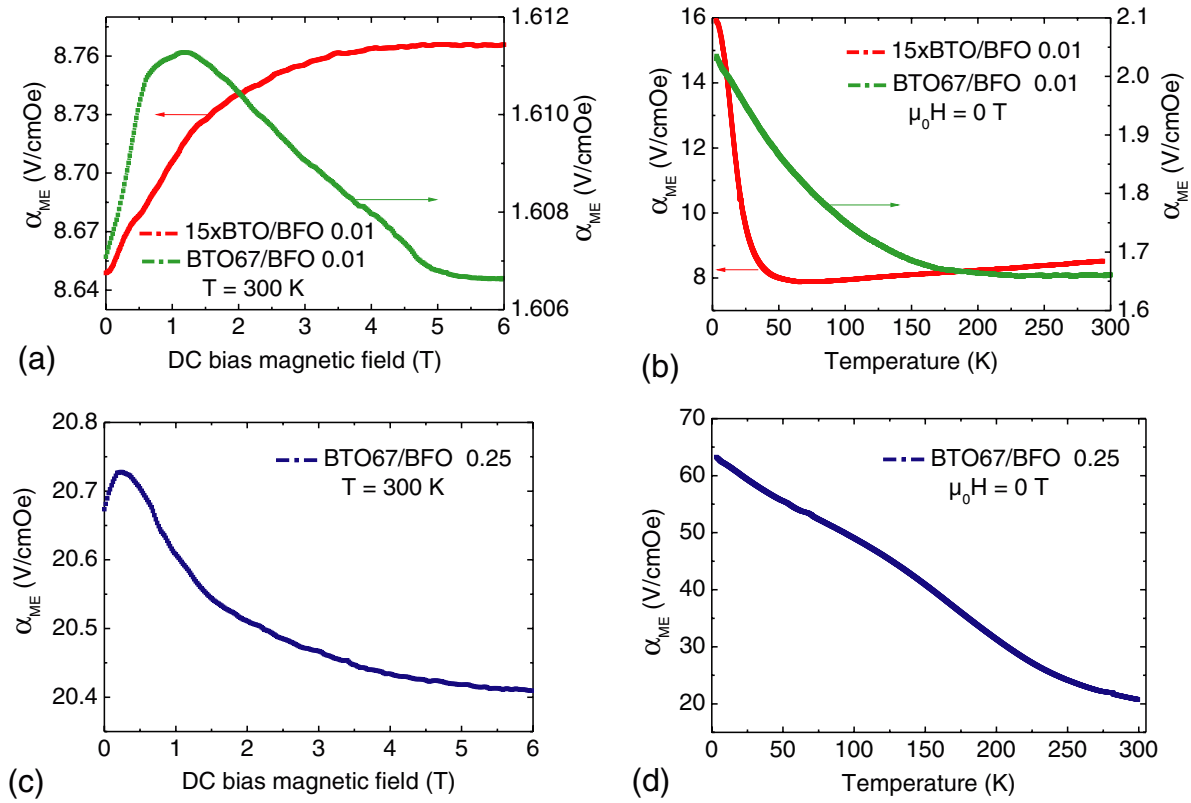

Figure 8. ME coefficient α_{ME} as a function of DC magnetic field (at 300 K) and temperature (at 0 T) for (*a*), (*b*) 15× BTO/BFO multilayer and BTO67/BFO33 composite thin films both grown at 0.01 mbar and (*c*), (*d*) BTO67/BFO33 composite film grown at 0.25 mbar, respectively.

References

Aimon N M, Kim D H, Choi H K and Ross C A 2012 Deposition of epitaxial $BiFeO_3/CoFe_2O_4$ nanocomposites on (0 0 1) $SrTiO_3$ by combinatorial pulsed laser deposition *Appl. Phys. Lett.* **100** 092901

Bary'achtar V G, L'vov V A and Jablonskii D A 1983 Theory of inhomogeneous magnetoelectric effect *JETP Lett.* **37** 673

Bern F, Schwinkendorf P, Setzer A, Lorenz M, Grundmann M, Vrejoiu I and Ziese M 2014 Magnetodielectric properties of $Pr_{0.7}Ca_{0.3}MnO_3$ films *J. Phys. Condens. Matter* submitted

Ding B-F and Zhou S-Q 2011 The coexistence of ferroelectricity and ferromagnetism in Mn-doped $BaTiO_3$ thin films *Chin. Phys.* B **20** 127701

Caicedo J M, Zapata J A, Gómez M E and Prieto P 2008 Magnetoelectric coefficient in $BiFeO_3$ compounds *J. Appl. Phys.* **103** 07E306

Catalan G and Scott J F 2009 Physics and applications of bismuth ferrite *Adv. Mater.* **21** 2463–85

Cao D, Cai M Q, Zheng Yue and Hua W Y 2009 First-principles study for vacancy-induced magnetism in nonmagnetic ferroelectric $BaTiO_3$ *Phys. Chem. Chem. Phys.* **11** 10934–8

Chu Y H *et al* 2007 Ferroelectric size effects in multiferroic $BiFeO_3$ thin films *Appl. Phys. Lett.* **90** 252906

Chu Y-H *et al* 2008 Electric-field control of local ferromagnetism using a magnetoelectric multiferroic *Nature Mater.* **7** 478

Dix N, Muralidharan R, Guyonnet J, Warot-Fonrose B, Varela M, Paruch P, Sánchez F and Fontcuberta J 2009 On the strain coupling across vertical interfaces of switchable $BiFeO_3$–$CoFe_2O_4$ multiferroic nanostructures *Appl. Phys. Lett.* **95** 062907

Doolittle L R 1985 Algorithms for the rapid simulation for Rutherford backscattering spectra *Nucl. Instrum. Methods Phys. Res.* B **9** 344–51

Dong S X, Zhai J Y, Li J-F and Viehland D 2006 Near-Ideal Magnetoelectricity in high-permeability magnetostrictive/piezofiber laminates with a (2-1) connectivity *Appl. Phys. Lett.* **89** 252904

Gruverman A, Auciello O and Tokumoto H 1998 Imaging and control of domain structures in ferroelectric thin films via scanning force microscopy *Annu. Rev. Mater. Sci.* **28** 101–23

Hong S, Woo J, Shin H, Jeon J-U, Pak Y E, Colla E L, Setter N, Kim E and No K 2001 Principle of ferroelectric domain imaging using atomic force microscope *J. Appl. Phys.* **89** 1377–86

Ivanov M S, Sherstyuk N E, Mishina E D, Sigov A S, Mukhortov V M and Moshnyaga V T 2012 Enhanced magnetization and ferroelectric switching in multiferroic BST/BNFO superstructures *Ferroelectrics* **433** 158

Khalid M *et al* 2009 Defect-induced magnetic order in pure ZnO films *Phys. Rev.* B **80** 035331

Lawes G and Srinivasan G 2011 Introduction to magnetoelectric coupling and multiferroic films *J. Phys. D: Appl. Phys.* **44** 243001

Lazenka V V, Lorenz M, Modarresi H, Brachwitz K, Schwinkendorf P, Böntgen T, Vanacken J, Ziese M, Grundmann M and Moshchalkov V V 2013 Effect of rare-earth ion doping on the multiferroic properties of $BiFeO_3$ thin films grown epitaxially on SrTiO3(1 0 0) *J. Phys. D: Appl. Phys.* **46** 175006

Lazenka V V, Zhang G, Vanacken J, Makoed I I, Ravinski A F and Moshchalkov V V 2012 Structural transformation and magnetoelectric behavior in $Bi_{1-x}Gd_xFeO_3$ multiferroics *J. Phys. D: Appl. Phys.* **45** 125002

Li M, Ning M, Ma Y, Wu Q and Ong C K 2007 Room temperature ferroelectric, ferromagnetic and magnetoelectric properties of Ba-doped $BiFeO_3$ thin films *J. Phys. D: Appl. Phys.* **40** 1603–7

Liu B, Sun T, He J and Dravid V P 2010 Sol–Gel-derived epitaxial nanocomposite thin films with large sharp magnetoelectric effect *ACS Nano* **4** 6836–42

Lorenz M, Hochmuth H, Schallner M, Heidinger R, Spemann D and Grundmann M 2003 Dielectric properties of Fe-doped $Ba_xSr_{1-x}TiO_3$ thin films on polycrystalline substrates at temperatures between −35 and +85 °C *Solid-State Electron.* **47** 2199–203

Lorenz M 2008 Pulsed laser deposition of ZnO-based thin films *Transparent Conductive Zinc Oxide. Basics and Applications in Thin Film Solar Cells* (*Springer Series in Materials Science* vol 104) ed K Ellmer *et al* (Berlin: Springer) pp 303–58 chapter 7

Lorenz M, Ziese M, Wagner G, Lenzner J, Kranert C, Brachwitz K, Hochmuth H, Esquinazi P and Grundmann M 2012 Exchange bias and magnetodielectric coupling effects in $ZnFe_2O_4$–$BaTiO_3$ composite thin films *CrystEngComm* **14** 6477–86

Lorenz M and Rao R (guest ed) 2014 Special issue 25 years of pulsed laser deposition *J. Phys. D. Appl. Phys.* **47** 030301

Ma J, Hu J, Li Z and Nan C-W 2011 Recent progress in multiferroic magnetoelectric composites: from bulk to thin films *Adv. Mater.* **23** 1062

Pabst G W, Martin L W, Chu Y-H and Ramesh R 2007 Leakage mechanisms in $BiFeO_3$ thin films *Appl. Phys. Lett.* **90** 072902

Sosnowska I, Peterlin-Neumaier T and Steichele E 1982 Spiral magnetic ordering in bismuth ferrite *J. Phys. C: Solid State Phys.* **15** 4835

Sundaresan A and Rao C N R 2009 Ferromagnetism as a universal feature of inorganic nanoparticles *Nano Today* **4** 96–106

Toupet H, Shvartsman V V, LeMarrec F, Borisov P, Kleemann W and Karkut M 2008 Enhanced magnetization in $BiFeO_3$/$BaTiO_3$ multilayers: an interface effect? *Integr. Ferroelectr.* **100** 165–76

Vaz C A F 2012 Electric field control of magnetism in multiferroic heterostructures *J. Phys.: Condens. Matter* **24** 333201

Wang J *et al* 2003 Epitaxial $BiFeO_3$ multiferroic thin film heterostructures *Science* **299** 1719

Weal E, Patnaik S, Bi Z, Wang H, Fix T, Kursumovic A and MacManus Driscoll J L 2010 Coexistence of strong ferromagnetism and polar switching at room temperature in $Fe3O_4$–$BiFeO_3$ nanocomposite thin films *Appl. Phys. Lett.* **97** 153121

Wu S M, Cybart S A, Yu P, Rossell M D, Zhang J X, Ramesh R and Dynes R C 2010 Reversible electric control of exchange bias in a multiferroic field-effect device *Nature Mater.* **9** 756

Zavaliche F *et al* 2005 Electric field-induced magnetization switching in epitaxial columnar nanostructures *Nano Lett.* **5** 1793–6

Zhan Q, Yu R, Crane S P, Zheng H, Kisielowski C and Ramesh R 2006 Structure and interface chemistry of perovskite–spinel nanocomposite thin films *Appl. Phys. Lett.* **89** 172902

Zheng H, Straub F, Zhan Q, Yang P-L, Hsieh W-K, Zavaliche F, Chu Y-H, Dahmen U and Ramesh R 2006 Self-assembled growth of $BiFeO_3$–$CoFe_2O_4$ nanostructures *Adv. Mater.* **18** 2747–52

Zippel J, Lorenz M, Setzer A, Rothermel M, Spemann D, Esquinazi P, Grundmann M, Wagner G, Denecke R and Timopheev A A 2013 Defect-induced magnetism in homoepitaxial manganese-stabilized zirconia thin films *J. Phys. D: Appl. Phys.* **46** 275002